Mutual Interference Mitigation in PMCW Automotive Radar

Zahra Esmaeilbeig[#], Arindam Bose^{*}, Mojtaba Soltanalian[#]

"WaveOPT Lab, University of Illinois Chicago, USA

"KMB Telematics, Inc, USA

{zesmae2, msol}@uic.edu, abose@kmb.ac

Abstract - This paper addresses the challenge of mutual interference (MI) in phase-modulated continuous wave (PMCW) millimeter-wave (mmWave) automotive radar systems. The increasing demand for advanced driver assistance systems (ADAS) has led to a proliferation of vehicles equipped with mmWave radar systems that operate in the same frequency band, resulting in MI that can degrade radar performance creating safety hazards. We consider scenarios involving two similar PMCW radar systems and propose an effective technique for a cooperative design of transmit waveforms such that the MI between them is minimized. The proposed approach is numerically evaluated via simulations of a mmWave automotive radar system. The results demonstrate that the proposed technique notably reduces MI and enhances radar detection performance while imposing very little computational cost and a negligible impact on existing infrastructure in practical automotive radar systems.

Keywords — Automotive radar systems, MIMO, mutual interference mitigation, PMCW, slow-time coding.

I. Introduction

Millimeter-wave (mmWave) automotive radar systems have gained significant attention due to their accurate object detection capabilities in challenging environments. Compared to cameras and Lidar, mmWave radar systems excel in heavy rain, fog, snow, and smoke [1], [2]. Operating within the 77 GHz to 81 GHz frequency range, these systems utilize high-frequency continuous waves (CW) for object detection. However, their poor angular resolution limits the detection of fine spatial details. Multiple-input multiple-output (MIMO) technology can improve the resolution, but it also introduces mutual interference (MI) challenges.

MI arises in MIMO radar systems when multiple transmitters operate in close proximity, leading to increased noise floor and reduced detection accuracy and reliability. Advanced signal processing techniques such as digital beamforming and adaptive filtering can mitigate this issue [3]. As the number of radar systems in vehicles grows and the mmWave frequency band becomes more congested, MI becomes increasingly problematic [4]. Modulation techniques, such as phase-modulated continuous wave (PMCW) and orthogonal frequency-division multiplexing (OFDM), offer advantages over traditional frequency-modulated continuous wave (FMCW), but they require higher sampling rates and sophisticated transceiver hardware [5].

Research in MI mitigation has focused on waveform design for FMCW radar systems [6], [7], [8], [9], [10].

Adaptive waveforms applied in slow-time or fast-time signals have been proposed, including slow-time coded waveforms, fast-generating adaptive slow-time coding schemes, and fast-time coding schemes [11]. Pseudo-orthogonal noise waveforms and specialized slow-time waveforms like the golden code and the linear frequency modulated CAZAC code have also been explored [8], [9], [10].

This paper focuses on mitigating MI among PMCW radars. While studies have addressed MI between FMCW and PMCW radars (see [12], [13], [14], [15] and the references within), there is a research gap in waveform design for PMCW systems, especially when radar systems possess similar physical parameters. A novel framework for designing collaborative waveforms is proposed to address this gap. The framework can handle non-convex objectives, is computationally efficient for practical implementation, and requires minimal modifications to the transceiver infrastructure.

II. PROBLEM FORMULATION

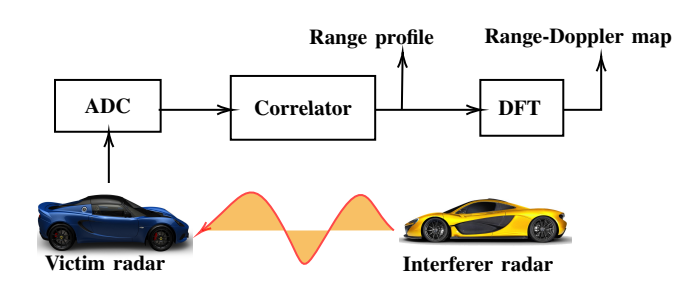


Fig. 1. Simplified illustration of the PMCW radar operation and PMCW-PMCW MI between two vehicles.

A. PMCW Signal Model

In this section, we formulate the PMCW radar model. We consider two PMCW automotive radar systems, depicted in Fig. 1, which are similar and mutually cooperative. These radars operate within the same frequency band. The transmit signal of both PMCW radars in a single *burst* of the signal can be described as

$$s(t) = \exp(j(2\pi f_c t + \phi(t))), \ 0 \le t \le T,$$
 (1)

where f_c is the carrier frequency, T is the pulse repetition interval (PRI) and $\phi(t)$ is the modulation phase waveform [4]. If the *chip* duration is T_c , then we denote the phase shift of the k-th chip by $x_k = e^{\mathrm{j}\phi(t)}$ for t in the interval $kT_c \leq t \leq (k+1)$

 $1)T_c$, resulting in $s(t)=\sum_{k=0}^{K-1}x_k\exp(\mathrm{j}2\pi f_ct)\mathrm{rect}\left(\frac{t-kT_c}{T_c}\right)$. We assume that N bursts of the signal is transmitted in one coherent processing interval (CPI). Therefore, the transmitted signal is

$$S(t) = \frac{1}{N} \sum_{n=0}^{N-1} s(t - nT)$$

$$= \frac{1}{N} \sum_{n=0}^{N-1} \sum_{k=0}^{K-1} x_k e^{j2\pi f_c t} \operatorname{rect}\left(\frac{t - kT_c - nT}{T_c}\right), \quad (2)$$

where $0 \le t \le NT$, and

$$\operatorname{rect}(t) = \begin{cases} 1 & 0 \le t \le 1, \\ 0 & \text{otherwise.} \end{cases}$$
 (3)

We consider a single target, located at range R and moving with velocity v towards the radar, which reflects back the radar signal. The two-way target propagation delay is $\tau_{\scriptscriptstyle T}(t)=\frac{2(R-vt)}{c}=\gamma_{\scriptscriptstyle T}-\frac{2v}{c}t$, where c is the speed of light. The received signal is

$$S_R(t) = \alpha_T S(t - \tau_T(t))$$

$$\approx \frac{\alpha_T}{N} e^{j2\pi f_c t} e^{-j2\pi f_c \gamma_T} e^{j2\pi f_c \frac{2v}{c} t} \times$$

$$\sum_{n=0}^{N-1} \sum_{k=0}^{K-1} x_k \operatorname{rect}\left(\frac{t - \gamma_T - kT_c - nT}{T_c}\right), \quad (4)$$

where we assumed $v \ll c$ for the approximation. We assume the cooperative performance of the two radars eliminates the carrier frequency offset (CFO) in the receiver. After mixing the received signal $S_R(t)$ with the conjugate of the carrier frequency, we assume the term $e^{-\mathrm{j}2\pi f_c\gamma_T}$ is absorbed in α_T . We denote $f_{d,T}=\frac{2v}{c}f_c$ as the Doppler frequency to obtain

$$\hat{S}_{R}(t) = \frac{\alpha_{T}}{N} e^{j2\pi f_{d,T} t} \sum_{n=0}^{N-1} \sum_{k=0}^{K-1} x_{k} \operatorname{rect}\left(\frac{t - \gamma_{T} - kT_{c} - nT}{T_{c}}\right).$$
(5)

As illustrated in Fig. 1, in the ADC, the time is split into fast time t' and slow time index n, with time interval T as t=t'+nT, $t'\in[0,T)$. In the fast-time, the signal can be sampled with interval T_c , i.e., at $t'=mT_c$, to obtain

$$\begin{split} r_{T}[m,n] &= \hat{S}_{R} \left(mT_{c} + nT \right) \\ &= \alpha_{T} e^{\mathrm{j}2\pi f_{d,T} (mT_{c} + nT)} \sum_{k=0}^{K-1} x_{k} \mathrm{rect} \left(\frac{(m-k)T_{c} - \gamma_{T}}{T_{c}} \right) \\ &= \alpha_{T} e^{\mathrm{j}2\pi f_{d,T} (mT_{c} + nT)} \sum_{k=0}^{K-1} x_{k} \delta_{m-\hat{n}_{T},k} \\ &= \alpha_{T} e^{\mathrm{j}2\pi f_{d,T} (mT_{c} + nT)} x_{m-\hat{n}_{T}}, \end{split} \tag{6}$$

where $\delta_{i,j}$ is the Kronecker delta function with $\hat{n}_T = \lfloor \frac{\gamma_T}{T_c} \rfloor$ is the number of code shifts due to the target at a range R. As illustrated in Fig. 1, in the receiver, the discrete signal in (6) will go through the correlator to yield the range profiles. The correlation between (6) and (2) is

$$r_{\scriptscriptstyle T}[m,n] = \alpha_T \sum_{k=0}^{K-1} x_k^* x_{k-\hat{n}_T+m} e^{\mathrm{j}2\pi f_{d,T}((m+k)T_c+nT)}, \quad (7)$$

which is the range profile of the target [13]. The impact of the second radar, acting as an interferer, on the range profile observed in the victim radar is represented in the following model.

B. Mutual Interference Model

The victim radar system receives a signal from the interferer radar transmitter that can be falsely interpreted by the receiver as a reflected signal from a target. Such interference when the two radars are transmitting PMCW is referred to as PMCW-PMCW interference [16]. In this section, the interferer PMCW radar system, transmitting signal with phase code $\mathbf{y} = [y_0, \dots, y_{K-1}]^{\top}$, similar to (2) is assumed to interfere with the victim radar transmitting PMCW signal with phase code $\mathbf{x} = [x_0, \dots, x_{K-1}]^{\top}$. We define the one-way delay associated with the interference as $\tau_I(t) = \frac{(R_I - v_I t)}{c} = \gamma_I - \frac{v_I}{c}t$, where R_I is the distance between two radar systems and v_I is the relative velocity between the two. Let $f_{d,I} = \frac{v_I}{c}f_c$ be the Doppler frequency associated with the interference. The interference samples in the receiver of the victim radar are

$$r_{I}[m,n] = \alpha_{I} \sum_{k=0}^{K-1} x_{k}^{*} y_{k-\hat{n}_{I}+m} e^{j2\pi f_{d,I}((m+k)T_{c}+nT)}$$
 (8)

with $\hat{n}_I = \lfloor \frac{\gamma_I}{T_c} \rfloor$ being the number of code shifts due to interference. It is worth highlighting that the cooperative performance of the two radars allows us to compensate for the desynchronization and differing PRI between them effectively.

III. MUTUAL INTERFERENCE MITIGATION

The received signal is formulated as

$$r[m,n] = r_{T}[m,n] + r_{I}[m,n] + w[m,n]$$

$$= \alpha_{T} \sum_{k=0}^{K-1} x_{k}^{*} x_{k-\hat{n}_{T}+m} e^{j2\pi f_{d,T}((m+k)T_{c}+nT)}$$

$$+ \alpha_{I} \sum_{k=0}^{K-1} x_{k}^{*} y_{k-\hat{n}_{I}+m} e^{j2\pi f_{d,I}((m+k)T_{c}+nT)} + w[m,n], \quad (9)$$

where w[m,n] represents the signal-independent disturbance, e.g., the receiver noise. In the receiver, (9) will go through the Doppler processor by applying the discrete Fourier transform (DFT) to the slow-time samples. As a result, the range-Doppler (RD) map is

$$\begin{aligned} \text{RD}[m,p] &= \alpha_T D_N \left(\tilde{f}_{d,T} - p/N \right) \sum_{k=0}^{K-1} x_k^* x_{k-\hat{n}_T + m} e^{\mathrm{j} 2\pi f_{d,T} (m+k) T_c} \\ &+ \alpha_I D_N \left(\tilde{f}_{d,I} - p/N \right) \sum_{k=0}^{K-1} x_k^* y_{k-\hat{n}_I + m} e^{\mathrm{j} 2\pi f_{d,I} (m+k) T_c} + W[m,p] \end{aligned}$$
(10)

where $\tilde{f}_{d,T} = f_{d,T}T$, $\tilde{f}_{d,I} = f_{d,I}T$ and $D_n(x) = \frac{sin(n\pi x)}{(\pi x)}$ is the Dirichlet function. A moving target changes the phases of the chips. This phenomenon is indicated by the $e^{j2\pi f_{\cdot,\cdot}(m+k)T_c}$ terms in (10). As a result, the received sequence will not be a pure binary sequence. This sensitivity to Doppler-induced phaseshift known as *Doppler intolerance* [18] creates small

sidelobes along the range profile as shown in Fig. 2a. It is also readily known that, for PMCW radars, the RD estimations are not coupled [13].

As mentioned in [12], the typical Doppler frequency is very low compared to the time scale of fast-time processing i.e. $f_{d,I} \ll 1/T_c$. It is evident from (10), that the interference is scaled by the cross-correlations in each range bin. We define

$$r_{xy}^{l}(f) = \sum_{k=0}^{K-1} x_{k}^{*} y_{(k+l) \bmod K} e^{j2\pi kf}$$
 (11)

and $\hat{f}_{d,I} = f_{d,I} T_c$. One can verify from (10) that $|r_{xy}^l(\hat{f}_{d,I})|$ for $l = m - \hat{n}_I$ is a dominant interfering term. In order to mitigate the MI between the two radar systems, we propose to suppress the interference power $|r_{xy}^l(\hat{f}_{d,I})|^2$. Hence, we consider the following optimization problem with respect to the two codes \mathbf{x} and \mathbf{y} :

$$\mathcal{P}_1: \underset{\mathbf{x}, \mathbf{y}}{\text{minimize}} \quad |r_{xy}^l(f)|^2$$
 subject to $|x_k|=1, \ |y_k|=1, \ \forall \, k.$ (12)

In practical scenarios, the victim and interferer radar on vehicles have asynchronous transmission and neither $\hat{n}_{\scriptscriptstyle I}$ nor $\hat{f}_{d,I}$ are known. Therefore, we seek to minimize interference on multiple grid points as

$$\mathcal{P}_2: \underset{\mathbf{x}, \mathbf{y}}{\text{minimize}} \sum_{l=-(L)}^{L} \sum_{p=-P}^{P} |r_{xy}^l(f_p)|^2$$
subject to $|x_k| = 1, |y_k| = 1, \forall k.$ (13)

The value of P is governed by the maximum Doppler frequency of interest. The range of the interference causing the code-shift \hat{n}_I affects many range bins according to the relation $l=m-\hat{n}_I$, therefore we choose a large enough L in order to mitigate the effect of interference in all range bins.

Remark 1. The expression in (11) may be recast as

$$r_{xy}^{l}(f_p) = \mathbf{x}^{\mathrm{H}} \mathrm{Diag}(\mathbf{f}_p) \, \mathbf{C}_l \mathbf{y}$$
 (14)

where $\mathbf{f}_p = [1, e^{\mathrm{j} 2\pi f_p}, \dots, e^{\mathrm{j} 2\pi (K-1) f_p}]^{\top}$ and

$$\mathbf{C}_{l} = \mathbf{C}_{-l}^{H} = \begin{bmatrix} \mathbf{0} & \mathbf{I}_{K-l} \\ \mathbf{I}_{l} & \mathbf{0} \end{bmatrix}. \tag{15}$$

The optimization problem (13) is non-convex due to the unimodularity constraints. Herein, we propose to tackle the problem in a cyclic manner. Specifically, in the s-th iteration of our cyclic optimization algorithm , we first optimize \mathbf{x} for fixed $\mathbf{y}^{(s-1)}$ and set the optimal solution as $\mathbf{x}^{(s)}$. Then, ceteris paribus, we optimize \mathbf{y} for fixed $\mathbf{x}^{(s-1)}$. In the following, we present the solution to the two sub-problems involved in each iteration. But first, we remark on the unimodular quadratic programs (UQPs) and the power-method-like (PMLI) iterations to tackle such problems.

Remark 2. A UQP is defined as

$$\underset{\mathbf{x} \in \Omega^K}{\text{maximize}} \quad \mathbf{x}^{H} \mathbf{G} \mathbf{x}, \tag{16}$$

where $\Omega^K = \{\mathbf{x} | x_k = e^{\mathrm{j}\omega}, \omega \in [0, 2\pi), k \in \{0, \dots, K-1\}\}$ is the set of unimodular vectors. The sequence of unimodular vectors at the s-th PMLI iteration

$$\mathbf{x}^{(s+1)} = e^{\mathrm{jarg}\left(\mathbf{G}\mathbf{x}^{(s)}\right)},\tag{17}$$

leads to a monotonically increasing objective value for the UQP, when G is a positive definite matrix. Moreover, in a UQP the diagonal loading technique is used to ensure the positive definiteness of the matrix, without changing the optimal solution. Particularly, in (16), the diagonal loading as $\widetilde{G} \leftarrow \lambda_m \mathbf{I} - \mathbf{G}$, with λ_m being slightly larger than the maximum eigenvalue of G, results in an equivalent problem and leaves us with a positive definite \widetilde{G} [19].

• Optimization of x for a fixed y: By substituting (14) in (13), the associated problem becomes

$$\mathcal{P}_3$$
: minimize $\mathbf{x}^{\mathrm{H}} \mathbf{B}_y \mathbf{x}$
subject to $|x_k| = 1, \forall k,$ (18)

where

$$\mathbf{B}_{y} = \sum_{l=-(L)}^{L} \sum_{p=-P}^{P} \operatorname{Diag}(\mathbf{f}_{p}) \mathbf{C}_{l} \mathbf{y} \mathbf{y}^{H} \mathbf{C}_{l} \operatorname{Diag}(\mathbf{f}_{p})^{H}. \quad (19)$$

By the diagonal loading technique introduced in Remark 2, we have the positive definite matrix $\widetilde{\mathbf{B}}_y = \lambda_m \mathbf{I} - \mathbf{B}_y$ and obtain the equivalent problem

$$\mathcal{P'}_3$$
: maximize $\mathbf{x}^{\mathrm{H}}\widetilde{\mathbf{B}}_y\mathbf{x}$
subject to $|x_k|=1, \forall k$. (20)

• Optimization of y for a fixed x: The problem with respect to y, mutatis mutandis, is

$$\mathcal{P}_4 : \underset{\mathbf{y}}{\text{maximize}} \quad \mathbf{y}^{\mathrm{H}} \widetilde{\mathbf{B}}_x \mathbf{y}$$

$$\text{subject to} \quad |y_k| = 1, \forall k$$
(21)

where $\widetilde{\mathbf{B}}_x = \lambda_m \mathbf{I} - \mathbf{B}_x$, and

$$\mathbf{B}_{x} = \sum_{l=-L}^{L} \sum_{p=-P}^{P} \operatorname{Diag}(\mathbf{f}_{p}) \mathbf{C}_{l} \mathbf{x} \mathbf{x}^{H} \mathbf{C}_{l} \operatorname{Diag}(\mathbf{f}_{p})^{H}.$$
 (22)

We cyclically optimize the subproblems \mathcal{P}'_3 and \mathcal{P}_4 , until convergence. Each of the subproblems is tackled by PMLI iterations introduced in Remark 2. The steps of the proposed algorithm are summarized in Algorithm 1. The objective value of (13) at iteration s is denoted by $J^{(s)}$.

In the following, we numerically evaluate the proposed algorithm.

IV. NUMERICAL EVALUATION

We consider two vehicles mounted with radars transmitting PMCW waveform operating at $f_c=79$ GHz and pulse duration of T=6.66 ns. N=140 burst of the signal is transmitted and a white Gaussian noise distributed as $\mathcal{N}(\mathbf{0}, 10^{-2}\mathbf{I})$ is added to the received signal, and target and interferer RCS are assumed to be 35 dBsm. The target is

Algorithm 1 PMCW waveform design for MI mitigation

```
Initialize: x^0, y^{(0)}, s = 0.
       Output: \mathbf{x}^*, \mathbf{y}^*. while |(J^{(s+1)}-J^{(s)})/J^{(s)}| \geq \epsilon do
 1:
                 Update \widetilde{\mathbf{B}}_{y}^{(s)}, t \leftarrow 0
 2:
                  \begin{array}{c} \textbf{repeat} \quad t \leftarrow t+1 \\ \mathbf{x}^{(s,t)} = e^{\mathrm{jarg}\left(\tilde{\mathbf{B}}_{y}^{(s)}\mathbf{x}^{(s,t-1)}\right)} \end{array} 
 3:
 4:
                 until convergence
 5:
                 \mathbf{x}^{(s)} \leftarrow \mathbf{x}^{(s,t)}
 6:
                 Update \widetilde{\mathbf{B}}_{x}^{(s)}, t \leftarrow 0
 7:
                 repeat t \leftarrow t+1
 8:
                          \mathbf{y}^{(s,t)} = e^{\mathrm{jarg}\left(\widetilde{\mathbf{B}}_x^{(s)}\mathbf{y}^{(s,t-1)}\right)}
 9:
                 until convergence
10:
                 \mathbf{y}^{(s)} \leftarrow \mathbf{y}^{(s,t)}
11:
12: end while
         return \mathbf{x}^* = \mathbf{x}^{(s)} and \mathbf{y}^* = \mathbf{y}^{(s)}.
```

placed at a range $R=20~\mathrm{m}$ and moving with velocity $v=30~\mathrm{m/s}$. The interferer radar is assumed to be located at a range $R_I=200~\mathrm{m}$ with relative velocity $v_I=-20~\mathrm{m/s}$. The 2D RDmap of the target scene, as seen in the victim radar, is illustrated in Fig. 2a and 2b for PMCW waveform with K=50 chips generated randomly and using Algorithm 1, respectively. One can observe that in Fig. 2a, the power of the interference is strong which leads to false alarm.

The optimized PMCW waveforms appear to effectively mitigate the interference and therefore improve the target detection performance of the radar.

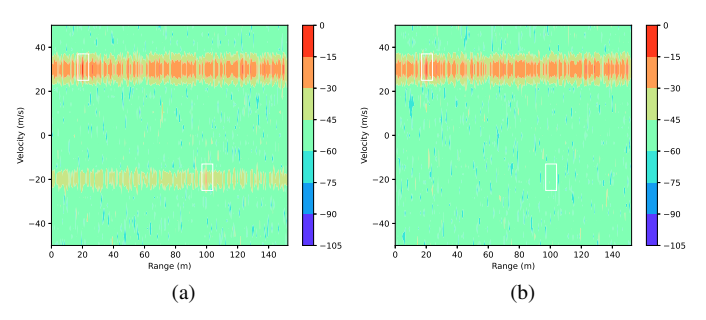


Fig. 2. RDmap of a single target with (a) random PMCW signal and (b) PMCW waveforms generated from Algorithm 1.

V. DISCUSSION

This paper examines the MI between two PMCW radars and introduces a cost-effective computational algorithm for designing transmit waveforms based on unimodular quadratic programming. The proposed algorithm demonstrates excellent performance when the two radars cooperate and share the designed waveform. Extending this research to automotive systems with a significant number of MIMO radars, where minimizing interference between any pair is crucial, represents an ongoing and highly desired challenge.

ACKNOWLEDGMENT

This work was sponsored by the National Science Foundation Grant ECCS-1809225.

REFERENCES

- F. Roos, J. Bechter, C. Knill, B. Schweizer, and C. Waldschmidt, "Radar sensors for autonomous driving: Modulation schemes and interference mitigation," *IEEE Microwave Magazine*, vol. 20, no. 9, pp. 58–72, 2019.
- [2] A. M. Elbir, K. V. Mishra, S. A. Vorobyov, and R. W. Heath, "Twenty-five years of advances in beamforming: From convex and nonconvex optimization to learning techniques," *IEEE Signal Processing Magazine*, vol. 40, no. 4, pp. 118–131, 2023.
- [3] T. Aittomäki and V. Koivunen, "MIMO radar filterbank design for interference mitigation," in *IEEE International Conference on Acoustics*, Speech and Signal Processing, 2014, pp. 5297–5301.
- [4] S. Alland, W. Stark, M. Ali, and M. Hegde, "Interference in automotive radar systems: Characteristics, mitigation techniques, and current and future research," *IEEE Signal Processing Magazine*, vol. 36, no. 5, pp. 45–59, 2019.
- [5] G. Hakobyan and B. Yang, "High-performance automotive radar: A review of signal processing algorithms and modulation schemes," *IEEE Signal Processing Magazine*, vol. 36, no. 5, pp. 32–44, 2019.
- [6] A. Bose, B. Tang, M. Soltanalian, and J. Li, "Mutual interference mitigation for multiple connected automotive radar systems," *IEEE Transactions on Vehicular Technology*, vol. 70, no. 10, pp. 11 062–11 066, 2021.
- [7] A. Bose, B. Tang, W. Huang, M. Soltanalian, and J. Li, "Waveform design for mutual interference mitigation in automotive radar," *arXiv* preprint arXiv:2208.04398, 2022.
- [8] Z. Xu and Q. Shi, "Interference mitigation for automotive radar using orthogonal noise waveforms," *IEEE Geoscience and Remote Sensing Letters*, vol. 15, no. 1, pp. 137–141, 2018.
- [9] J.-C. Belfiore, G. Rekaya, and E. Viterbo, "The golden code: a 2×2 full-rate space-time code with nonvanishing determinants," *IEEE Transactions on Information Theory*, vol. 51, no. 4, pp. 1432–1436, 2005.
- [10] S. Cao and N. Madsen, "Slow-time waveform design for MIMO GMTI radar using CAZAC sequences," in *IEEE Radar Conference*, 2018, pp. 1456–1460.
- [11] V. F. Mecca and J. L. Krolik, "Slow-time MIMO STAP with improved power efficiency," in Asilomar Conference on Signals, Systems and Computers, 2007, pp. 202–206.
- [12] H.-P. Beise, T. Stifter, and U. Schröder, "Virtual interference study for FMCW and PMCW radar," in *German Microwave Conference*. IEEE, 2018, pp. 351–354.
- [13] H. C. Yildirim, M. Bauduin, A. Bourdoux, and F. Horlin, "Impact of phase noise on mutual interference of FMCW and PMCW automotive radars," in *European Radar Conference*. IEEE, 2019, pp. 181–184.
- [14] A. Bourdoux, K. Parashar, and M. Bauduin, "Phenomenology of mutual interference of FMCW and PMCW automotive radars," in *IEEE Radar Conference*, 2017, pp. 1709–1714.
- [15] S. Xu and A. Yarovoy, "Doppler shifts mitigation for PMCW signals," in *International Radar Conference*. IEEE, 2019, pp. 1–5.
- [16] J. P. Bordes, C. Davis, W. E. Stark, O. A. Schmid, and R. K. Rao, "PMCW-PMCW interference mitigation," 2019, US Patent App. 16/443,205.
- [17] Z. Esmaeilbeig, A. Eamaz, K. V. Mishra, and M. Soltanalian, "Moving target detection via multi-IRS-aided OFDM radar," arXiv preprint arXiv:2302.12884, 2023.
- [18] R. M. Davis, R. L. Fante, and R. P. Perry, "Phase-coded waveforms for radar," *IEEE Transactions on Aerospace and Electronic Systems*, vol. 43, no. 1, pp. 401–408, 2007.
- [19] M. Soltanalian and P. Stoica, "Designing unimodular codes via quadratic optimization," *IEEE Transactions on Signal Processing*, vol. 62, no. 5, pp. 1221–1234, 2014.